Experimental Studies on Metallic Fuel Relocation in a Single-Pin Core Structure of a Sodium-Cooled Fast Reactor

Taeil Kim*, Dzmitry Harbaruk, Craig Gerardi, Mitchell Farmer, and Yoon Il Chang

Argonne National Laboratory, 9700 S Cass Ave, B206, Argonne, IL 60439, United States

Abstract

Experiments dropping molten uranium into test sections of single fuel pin geometry filled with sodium were conducted to investigate relocation behavior of metallic fuel in the core structures of sodium-cooled fast reactors during a hypothetical core disruptive accident. Metallic uranium was used as a fuel material and HT-9M was used as a fuel cladding material in the experiment in order to accurately mock-up the thermo-physical behavior of the relocation. The fuel cladding failed due to eutectic formation between the uranium and HT-9M for all experiments. The extent of the eutectic formation increased with increasing molten uranium temperature. Voids in the relocated fuel were observed for all experiments and were likely formed by sodium boiling in contact with the fuel. In one experiment, numerous fragments of the relocated fuel were found. It could be concluded that the injected metallic uranium fuel was fragmented and dispersed in the narrow coolant channel by sodium boiling.

Keywords: SFR, HCDA, Metal Fuel, Relocation, Eutectic Formation, Fragmentation

1. Introduction

The prototype generation-IV sodium cooled fast reactor (PGSFR) is being developed by Korea Atomic Energy Research Institute (KAERI) as a next generation nuclear reactor. The PGSFR design includes two main passive safety characteristics, a large sodium pool and a metal fuel core, that are expected to maintain core integrity in several postulated anticipated transient without scram (ATWS) events such as loss-of-flow without scram (LOFWS), loss-of-heat-sink without scram (LOHSWS), and transient overpower without scram (TOPWS). The combination of the thermal inertia of the large sodium pool and the high thermal conductivity of the metal fuel enable the reactor to passively shut down. This behavior was successfully demonstrated in the landmark shutdown heat removal test conducted in EBR-II [1].

However, it is still necessary to evaluate consequences of hypothetical core disruptive accidents (HCDAs) that may occur under ATWS events with conservative assumptions.

* Corresponding author. Tel.: +1 630 252 7450
E-mail addresses: tikim@anl.gov (T. Kim).

Extensive studies regarding fuel relocation behavior in case of the HCDAs under both in-pile and out-of-pile conditions were conducted for oxide fuels in the 1960s – 1970s, while only few studies of metal fuel relocation behavior were performed because of concerns that the metal fuel could not achieve high burnup due to the irradiation induced swelling problem [2]. Following the new metal fuel design development that overcame the swelling problem, experiments regarding thermal hydraulic interaction of molten metallic fuels and liquid sodium have been conducted by several researchers [3-9]. Nishimura et al. [3-5] carried out a series of fragmentation experiments using molten metallic simulants in a sodium pool. The simulant materials (Copper, Silver, and Aluminum) with quantities ranging from 20 g to 300 g were melted in a crucible with an electrical heater and were dropped into a sodium pool with temperatures from 206 °C to 500 °C. It was reported that the thermal fragmentation originated inside the molten simulants and a solid crust was observed. It was verified that the fragmentation of the molten simulants was attributed to the internal pressure build up by the boiling of sodium, which was locally entrapped inside the molten simulants due to turbulent mixing of the molten simulants and sodium. It was concluded that the superheating and the latent heat of fusion of a molten metal jet were dominant factors governing the thermal fragmentation. The effect of the initial temperature of the coolant sodium on the fragmentation of the simulants was found to be negligible. Zhang et al. [6] investigated the fragmentation of a single molten copper droplet (1g – 5 g) in a sodium pool with temperatures from 249 °C to 314 °C. They found intensive fragmentation of a single molten copper droplet even if the instantaneous contact temperature between the copper and the sodium was below the melting point of copper. They [7] continued to investigate the fragmentation characteristics of a single molten stainless steel droplet (1g – 5g) in a sodium pool with temperatures from 295 °C to 337 °C. The fine fragmentation of a single molten stainless steel droplet was confirmed again. Most studies that were conducted using metallic simulants in sodium concluded that the molten metals were heavily fragmented after liquid contact and the dominant factors governing the fragmentation were superheating and latent heat of fusion of the simulants. Gabor et al. conducted experiments using kilogram quantities of various molten uranium alloys in an open sodium pool configuration [8, 9]. They found that the metal fuel fragments created from their pour stream in the open sodium pool were in the form of filaments and sheets with a high bed voidage on the order of 0.9. Their calculation indicated that the debris beds formed by relocated metal fuels in an open sodium pool would be largely coolable by conduction heat transfer; and even if deep beds were to form, convective heat transfer and boiling heat transfer could preclude further melt penetration. Although Gabor et al.'s experiments are useful in evaluating the coolability of relocated metal fuels during the HCDAs in a SFR, they focused on the late phase relocation behavior in which the core material relocates downward through the core support plate into the inlet plenum where the structures are more open and thus consistent with the open pool configuration. There is still a knowledge gap regarding the initial phase of metal fuel relocation behavior within the core structures in case of the HCDAs.

Recently, studies regarding fuel discharge behavior through core coolant channels have been conducted by using metallic simulants with a low melting temperature [10, 11]. Kamiyama et al. [10] conducted a series of experiments injecting an alloy with a low melting temperature into a rectangular water channel. They observed the fuel discharge through the coolant channel with the void expansion of the coolant and concluded that the extent of discharge of the fuel was highly dependent on the hydraulic diameter of the channel. Heo et al. [11] also visually investigated fuel discharge behavior through a rectangular coolant channel by using gallium. They observed upward discharge of the gallium fuel simulant when R123 was used as a coolant. It was concluded that the vapor pressure build up by the boiling of the coolant was one of the driving forces for the upward discharge. Although these experimental works regarding the metal fuel discharge behavior showed a possibility of fuel exclusion from the core region at the initial phase of the HCDAs, further works are still necessary to understand the behavior of the metal fuel in a prototypical core structure.

In the present study, experiments were performed that dropped molten uranium fuel into test sections with a single fuel pin geometry filled with sodium. The geometry and materials used mocked-up the core structures of the PGSFR to understand the initial phase of relocation behavior of metallic fuel within the core region. Uranium metal was selected as a fuel material and HT-9M was selected as a cladding material to investigate the extent of eutectic formation between them in the core region. Simulant materials would not be able to capture this behavior accurately since eutectic formation is material specific. Posttest radiographic images were taken without draining the sodium to keep the frozen uranium in its final position. Finally, the temperature profile as a function of time at the eutectic formation region was numerically calculated to evaluate the moment of the cladding breach and the sodium boiling.

2. Experiments

2.1 Metallic Uranium Safety Experiment (MUSE) Facility

A schematic diagram of Argonne National Laboratory's Metallic Uranium Safety Experiment (MUSE) facility for metal fuel relocation experiments is shown in Figure 1. The MUSE facility consisted of a melt assembly, a single fuel pin test section with a vertical split tube furnace, a sodium transfer system, instrumentation and control, and a containment box. The melt assembly consisted of a graphite crucible, a plug and a rod, a pneumatic cylinder, an induction heater with a motor generator, an injection line, a diaphragm, and a melt vessel, which is shown in Figure 2. Both the crucible and the plug were coated by yttria since it is known as the most stable material available for the molten uranium. The metallic uranium fuel was inductively heated in the graphite crucible by a 30-kW,10-kHz motor generator powering a copper coil. The plug was removed pneumatically with the tantalum rod from the crucible, which permitted downward injection of the fuel melt. The single fuel pin test section was a mock-up of the core structures of the PGSFR and was installed at the bottom flange of the injection line of the melt assembly so

that the molten fuel could be injected into the test section. The test section was heated by the vertical split tube furnace to its desired temperature. The sodium transfer system consisted of a sodium supply tank filled with 15 kg of pure sodium, tank heaters and insulation, 316 stainless steel (SS) sodium line tubes, pneumatic valves, sodium line heaters, a sodium dump tank, and a vapor trap. All the fittings used in the transfer lines were 316 SS VCR fittings that were rated for 538 °C at 25.5 MPa.

2.2 Single Fuel Pin Test Section

The single fuel pin test section consisted of a containment tube, a zirconia tube, and a HT-9M cladding with alumina fillers, a funnel, thermocouples, and sodium level meters as shown in Figure 3. The containment tube was fabricated from a 316 SS tube. The zirconia was used as the outer diameter of the narrow coolant channel because zirconia is compatible with molten uranium and is a good insulator which acted as an adiabatic boundary during the initial relocation phase. The fuel cladding was fabricated from 7.4-mm outside diameter and 0.5-mm thickness of a HT-9M tube, and alumina was used to fill the inner diameter to prevent sodium from flowing inside the cladding. The gap between the fuel cladding and the zirconia tube was 1.865 mm, which was 3 times of hydraulic area compared to a single fuel pin subchannel of the PGSFR's core structure. The coolant channel in the PGSFR is not an annulus but interconnected, therefore the molten fuel injected into a PGSFR subchannel would be able to flow beyond the hydraulic area of a single fuel pin subchannel. This was why the gap in our experiments was chosen to have a larger hydraulic area.

There were a few differences between the designs of the two sections in order to study the impact of the fuel injection point on the eutectic and fragmentation behavior of the fuel. Test section #1 used a guide tube to direct the molten metal fuel into the fuel cladding, while the fuel cladding was extended to the bottom of the funnel in the test section #2. The inside surface of the guide tube was coated by yttria to prevent eutectic formation during fuel injection. A weak spot with a thickness of 0.0254 mm was fabricated on the cladding at different locations for the two test sections with the goal of controlling the fuel injection point into the sodium coolant channel. The weak point was located at the same height of the alumina filler for test section #1 and located at 25.4 mm above the alumina filler for test section #2. The selection of the location of the weak spot location is explained in the results and discussion (Section 3). The sodium level between the container tube and the zirconia tube was same as the height of the weak spot. The sodium level between the zirconia tube and the fuel cladding was higher than that between the container tube and the zirconia tube due to a capillary action, which was confirmed by posttest radiographic images. The test section thermocouple 1 (TC1) was inserted into the route of the molten uranium to measure the uranium temperature directly. Additional test section thermocouples (TC2 – TC11) were installed on the outside surface of the zirconia tube for the test section #1. For test section #2, TC2 – TC5 were installed at the inner surface of the zirconia

tube to directly measure the temperature of sodium in the coolant channel, while TC6 – TC11 were installed on the outside surface of the zirconia tube.

2.3 Experimental Procedure and Conditions

The experimental procedure was as follows. The melt assembly, the test section, and the sodium transfer system were evacuated by using a vacuum pump and purged by argon gas to remove air and moisture in the MUSE facility. Afterwards, the test section and the sodium transfer system were heated to 250 °C to avoid the solidification of the sodium during transfer from the sodium supply tank to the test section. The sodium was transferred by pressurizing the sodium supply tank to 10 psia. Following sodium transfer, the test section was heated up to its desired temperature by the vertical split tube furnace. After the sodium filling process in the test section, the uranium fuel was heated inductively to its desired temperature in the graphite crucible. The molten uranium metal was then dropped through the injection line to the diaphragm by using the pneumatic cylinder. Once the diaphragm melted, which was nearly instantaneous, the molten fuel was directed into the guide tube and the fuel cladding by the funnel. Posttest radiographic images were taken without draining of the sodium to investigate the relocation of metal fuel in the test section.

Two principal mechanisms have been identified as causing fuel cladding damage in metal fuels; pin plenum overpressure by fission gas/bond sodium vapor and clad thinning by eutectic formation [12]. When the fuel cladding fails, overpressure results in a high ejection velocity of molten fuel which is beneficial for the fragmentation and the dispersion of the molten fuel. However, for a low initial fuel burnup condition, the pin plenum pressure is expected to be low and thus the ejection velocity is expected to be low too. In the present study, the characteristics of relocation behavior of the metal fuel in a narrow sodium channel was investigated under a conservative condition of a low ejection velocity less than 2 m/s and a low Weber number less than 10, which was consistent with a low burnup condition [12]. Iron-uranium eutectic formation temperature was expected to occur in the range of 700 °C to 1100 °C, and the threshold value where eutectic formation becomes very rapid was expected at approximately 1080 °C [13]. Uranium metal was selected as a fuel material and HT-9M was selected as a cladding material to investigate the extent of eutectic formation between them in the core region. Recently, sodium coolant temperature was calculated by MARS-LMR code for ATWS events of the PGSFR [14]. The peak coolant temperature was reported as 670 °C for TOPWS, 620 °C for LOHSWS, and 880 °C for LOFWS. Tentner et al. also conducted the analysis of severe accidents of the PGSFR by using the SAS4A code [15]. The peak fuel temperature was reported above 1400 °C for LOF-TOPWS. Based on this information, the initial temperature of uranium at TC1 of the test section was varied from 1248 °C to 1333 °C and the sodium temperature near the weak spot was varied from 501 °C to 622 °C. The amount of fuel material used for experiment #1 and experiment #2 was 212.37 g and 308.76 g, respectively. The parameters for the metal fuel relocation experiments are summarized in Table 1.

3. Results and Discussion

3.1 Metal Fuel Relocation Experiment #1

The metal fuel relocation experiment #1 was conducted with 212.37 g of pure depleted uranium metal. The uranium metal was heated inductively to 1565 °C, which was 433 °C higher than its melting temperature, in the graphite crucible with 35% of rated power of the induction generator. The temperature of uranium in the crucible was measured by a type C thermocouple with a 3.175-mm diameter. Afterwards, the molten uranium was dropped into the injection line by pneumatically lifting the bottom plug of the graphite crucible. The molten uranium failed the diaphragm and dropped into the single fuel pin test section. Test section #1 was used for experiment #1 and the temperature of test section #1 was monitored by 11 type K thermocouples (TC1–TC11) with a 1.5875-mm diameter. TC1 was inserted into the guide tube to directly measure uranium temperature. TC2 –TC11 were installed at the outside surface of zirconia tube. The responses of the thermocouples are shown in Figure 4. TC1 increased from 523 °C to 1248 °C 1.1 seconds after the bottom plug was lifted, which was interpreted as the time that the molten uranium passed TC1 in the guide tube. Additionally, this showed that the temperature of the molten uranium decreased more than 300 °C from its temperature in the graphite crucible. The heat loss was likely caused by heat conduction through the funnel after molten uranium contact. TC1 decreased from its maximum value of 1248 °C to 1004 °C after 2.7 seconds and decreased to 801 °C after 21.1 seconds. This rapid cooling of the uranium could be attributed to efficient heat transfer between the uranium, test section structure, and the sodium. It took more than 300 seconds for the uranium to become an equilibrium state. It should be noted that the maximum temperature of 1248 ˚C was at the upper limit of type K thermocouple (1250 ˚C). Therefore, a type R thermocouple with an upper limit of 1450 ˚C was used as TC1 in the experiment #2. TC2 and TC3 increased to their maximum temperature after 80 seconds and then decreased to their equilibrium state after 300 seconds. Meanwhile, TC4–TC11 experienced a small temperature peak after few seconds from the drop moment and entered into their equilibrium state within 10 seconds from the drop moment. This different temperature behavior between TC2 – TC3 and TC4 – TC11 indicated that the molten uranium flowed only to the height of TC3, which was confirmed by the radiographic image. The small peak showed in TC4 – TC11 was probably due to the small amount of uranium dropped into the outer annular channel between the container tube and the zirconia tube. This was not an intentional aspect of the experiment and was likely due to uranium splashing from the funnel. The total amount of uranium that went through outer annulus was estimated to be less than 5 g.

The pressure measurements of the test section and the melt assembly are displayed in Figure 5. In experiment #1, the melt vessel pressure and the test section pressure were matched at about atmospheric pressure to reduce any pressure induced splashing of molten uranium when the diaphragm was broken. The pressure of the melt vessel was 1.061 bar and the pressure of the test

section was 1.046 bar at the drop moment. After the molten uranium drop and the following break of the diaphragm, the test section pressure increased to 1.102 bar and maintained for about 4 seconds and decreased to 1.027 bar. This pressure increase in the test section was probably due to the boiling of the sodium. After the argon purge from the melt vessel to the sodium vent line was turned on at 7 seconds, both the melt vessel pressure and the test section pressure gradually increased to their equilibrium state.

The radiographic test was performed following experiment #1 without draining the sodium in order to keep the frozen uranium in its original position. The radiographic image of the test section showed that the most of uranium froze in the graphite funnel, the guide tube, and the HT-9 cladding as shown in Figure 6. Some uranium leaked through the gap between the funnel and the zirconia tube. The weak spot of the fuel cladding was broken by the molten uranium. The uranium was not fragmented near the weak spot but just froze and plugged directly outside of the weak spot in the annulus. The temperature of the uranium after failure of the weak spot was likely not high enough for the uranium to be fragmented in the narrow sodium channel due to heat loss. After the uranium froze and plugged the weak spot, the uranium dropped above this point accumulated in the cladding and the guide tube. Interestingly, a region of fuel cladding about 25.4 mm above the weak spot was deformed and broken through due to eutectic formation between the uranium and the HT-9 cladding. This corresponds to the round white region in the radiographic image and was likely formed by the boiling of sodium when the fuel cladding failed by eutectic formation. It was also found that some uranium flowed inside the coolant channel. The frozen sodium level was found in the radiographic image. The sodium level noted in the radiograph was just below TC5 although it was initially located near TC3 during the test. This discrepancy was resulted from the density difference of sodium between room temperature and 500 °C.

Test section #1 was uninstalled from the MUSE facility following the radiographic testing and disassembled as shown in Figure 7. First, the funnel and the fuel cladding with the zirconia tube were detached from the test section container tube. Second, the graphite funnel, the guide tube, and the fuel cladding were removed from the zirconia tube. It was confirmed that the fuel cladding was deformed and broken through due to the eutectic formation between the uranium and the HT-9M cladding. Some white spots near the eutectic formation region implied that sodium was filled to that height due to the capillary action. The close-up pictures of the eutectic formation region clearly showed the spherical voids formed by the boiling of the sodium. Also, 10-mm length of frozen uranium piece was found in the coolant channel.

3.2 Metal Fuel Relocation Experiment #2

Metal fuel relocation experiment #2 was conducted with 308.76 g of uranium metal. The uranium was initially heated to 1690 °C, which was 125 °C higher than in experiment #1. Test section #2 was used for the experiment #2 and the temperature of the test section was monitored by 1 type R thermocouple (TC1) and 10 type K thermocouples (TC2 –TC11). The location of the

weak spot was raised 25.4 mm from the alumina filler to increase the temperature of uranium when it was injected into the coolant channel. TC1 was inserted into the fuel cladding to directly measure uranium temperature. TC2 –TC5 were installed at the inner surface of the zirconia tube to directly measure the temperature of sodium in the coolant channel and uranium metal as it passes those junctions, while TC6 – TC7 were installed on the outside surface of the zirconia tube. The responses of the thermocouples are shown in Figure 8. TC1 increased from 607 °C to 1333 °C after 1.0 seconds from the release moment of molten uranium from the crucible. Afterwards, TC1 decreased from its maximum value of 1333 °C to 1000 °C after 4.6 seconds and decreased to 801 °C after 23.8 seconds. It took more than 400 seconds for the uranium to become an equilibrium state. Unlike experiment #1, TC2 experienced a temperature spike of more than 300°C and TC3 experienced a temperature spike of more than 100 °C, which indicates that much more uranium was injected into the coolant channel compared to experiment #1. Meanwhile, TC4 – TC11 experienced a small temperature peak after few seconds from the drop moment and entered into their equilibrium state within 10 seconds from the drop moment. This different temperature behavior between TC2 – TC3 and TC4 – TC11 implied again that the molten uranium flowed only to the height of TC3, which was confirmed by the radiographic image.

The radiographic images that were taken following experiment #2 without draining the sodium to keep the frozen uranium in its original position are shown in Figure 9. The radiographic images showed that the initial portion of uranium dropped into the fuel cladding froze above the alumina fillers below the weak spot. This uranium remained inside the fuel cladding and did not break the cladding by eutectic formation. It was found that the uranium that relocated to the region near and above the weak spot remained hot enough to fail the weak spot and portions of the fuel cladding above the weak spot. Most of the upper portion of the uranium did not remain inside the cladding and came out of the cladding by the eutectic formation. A large number of round shaped white spots inside the fuel cladding above the weak spot indicate that there was vigorous sodium boiling. The zirconia tube was broken probably due to the thermal shock induced by the temperature difference between the uranium and the zirconia tube. Due to the break of the zirconia tube, substantial amount of the uranium flowed into the outer channel between the container tube and the zirconia tube. The uranium that flowed into the outer channel was frozen as a lump because its temperature was not high enough to be fragmented. Some uranium leaked through the gap between the funnel and the container tube.

The pictures of the disassembled test section #2 are shown in Figure 10. Substantial eutectic formation between the uranium and the fuel cladding above the weak spot was confirmed. The uranium, fuel cladding, and the zirconia tube were stuck together and the shape of the fuel cladding was not recognizable due to the eutectic formation. Plenty of fragments of the uranium were found in the region above the weak spot and this was the evidence of fragmentation of the uranium in the coolant channel. The size of the fragments varied from less than 0.5 mm to more than 10 mm. The shape of the fragments was typically a flat sheet. The fragmentation of the uranium could be attributed to the vigorous sodium boiling. Below the weak spot, the fuel

cladding was intact and the uranium was frozen on the cladding surface. It was also confirmed that the uranium that flowed into the outer channel froze as a lump. It was evident that the uranium found above the weak spot was substantially more rough and porous than the uranium lump found in the outer channel.

3.3 Numerical Analysis

The temperature profile as a function of time at the eutectic formation region above the weak spot was numerically calculated to evaluate the breach moment of the fuel cladding and the instantaneous contact temperature. Assumptions were made for the numerical calculation as follows:

- The system was azimuthally symmetric and independent of z-direction.
- The uranium temperature at 12.7 mm above the weak spot was assumed same as the TC1 measurement.
- For the experiment #1, the zirconia tube outside temperature at 12.7 mm above the weak spot was an average value of the TC2 measurement and the TC3 measurement. This temperature was named as TC2.5.

A finite difference method was applied with these assumptions to the system shown in Figure 11. Introducing a mesh of nodes along the r-direction, r_i with i = 1, 2, …, and Δr = 0.1 mm between the uranium and the zirconia tube and a mesh of nodes in time t_j with j = 1, 2, …, spacing Δt = 0.00005 seconds, and forwarding difference in time, the finite difference analog is as follows:

$$\frac{T_{i,j+1} - T_{i,j}}{\Delta t} = \alpha \frac{r_{i+1/2}\left(\frac{T_{i+1,j} - T_{i,j}}{\Delta r}\right) - r_{i-1/2}\left(\frac{T_{i,j} - T_{i-1,j}}{\Delta r}\right)}{r_i \Delta r} \quad (1)$$

where T is a temperature, α is a thermal diffusivity, $r_{i+1/2}$ is a radial position located halfway between r_{i+1} and r_i, $r_{i-1/2}$ is a radial position located halfway between r_i and r_{i-1}. The Δt was selected to satisfy the Courant-Friedrich-Lewy (CFL) condition, namely:

$$\Delta t < \frac{\Delta r^2}{2\alpha} \quad (2)$$

The calculated temperature profile as a function of time at 12.7 mm above the weak spot was shown in Figure 12. It should be noted that the actual temperature behavior of the system would be different from the calculation results because sodium boiling was not considered. The calculated inside fuel cladding temperature exceeded the onset of eutectic formation point

(700 °C) at 0.52 seconds and 0.61 seconds for the experiment #1 and experiment #2, respectively. Then, it exceeded the threshold value (1080 °C) where the eutectic formation rate becomes very rapid at 0.95 seconds and 0.74 seconds for the experiment #1 and experiment #2, respectively. Based on the penetration rates measured by Walter and Kelman [13], about 1 second is necessary for the fuel cladding breach by the eutectic penetration. Consequently, the timing of the cladding breach was estimated as 1.95 seconds and 1.74 seconds for the experiment #1 and the experiment #2, respectively. TC2 in the experiment #2, which directly measured the coolant channel sodium temperature, experienced a temperature hike at 1.7 seconds and this indicates that the cladding breach occurred at 1.7 seconds. The calculated breach moment and measured breach moment were in a good agreement for the experiment #2. It was hard to find a similar temperature hike from the measurements in the experiment #1 because the thermocouples measured the temperature of the zirconia tube outside surface. Based on the numerical calculation, it could be concluded that the breach of the fuel cladding and the subsequent sodium boiling was occurred within few seconds from the drop moment.

The instantaneous contact temperature between the molten uranium and the sodium and the ambient Weber number at the cladding breach moment were calculated by using following equations [6]:

$$T_{instant\ contact} = \frac{T_{Na} + T_u \left(\frac{k_u \rho_u C_{p,u}}{k_{Na} \rho_{Na} C_{p,Na}}\right)^{1/2}}{1 + \left(\frac{k_u \rho_u C_{p,u}}{k_{Na} \rho_{Na} C_{p,Na}}\right)^{1/2}} \quad (3)$$

$$We_a = \frac{\rho_u v^2 D_o}{\sigma_u} \quad (4)$$

where k is a thermal conductivity, ρ is a density, C_p is a specific heat capacity, v is an injection velocity, D_o is an injection diameter, σ is a surface tension, a subscript Na means sodium and a subscript U means uranium. The measured uranium temperature by TC1 at the breach moment was 1061 °C and 1283 °C for the experiment #1 and the experiment #2, respectively. The measured coolant channel sodium temperature by TC2 in the experiment #2 showed that it didn't increase much until the fuel cladding was breached. Therefore, the coolant channel sodium temperature at the breach moment can be assumed as 501 °C and 622 °C for the experiment #1 and the experiment #2, respectively. The calculated instantaneous contact temperature was 710 °C and 869 °C for the experiment #1 and the experiment #2, respectively. And the weber number was calculated as 5.2 and 3.4 for the experiment #1 and the experiment #2 respectively. The instantaneous contact temperature of the previous studies [3-9], in which the fragmentation was observed, was mostly in the range of 800 °C to 1100 °C and weber number was mostly in the range of 20 to 200. The weber number of the present study was relatively low

compared to those of previous studies. The instantaneous contact temperature of the experiment #2 was in the range of 800 °C to 1100 °C, while it was not in that range for the experiment #1. The difference of the instantaneous contact temperature between the experiment #1 and the experiment #2 probably resulted in the difference of the occurrence of the fragmentation. The instantaneous contact temperature and the weber number of previous studies and present study are summarized in Table 2.

Generally, the instantaneous contact temperature of the present study was comparable to those of previous studies but the Weber number of present study was relatively small compared to those of previous studies due to the narrow sodium channel. It could be concluded that the injected metallic uranium fuel into the coolant channel is able to be fragmented and dispersed in the narrow coolant channel by the sodium boiling. Because the sodium channel geometry of the present study was not a pin bundle geometry but a single fuel pin geometry, only qualitative conclusions could be drawn regarding the relocation behavior of the molten uranium in the core region and further studies with a pin bundle geometry are necessary. It should be also noted that the molten fuel would be injected into the coolant channel with a back-pressure in a SFR HCDA due to the fission gas and the bond sodium vapor. This would promote the fragmentation and the dispersion of the molten fuel. Furthermore, greater penetration of the fuel into the lower core would increase negative reactivity feedback resulting in reactor shutdown. Further studies regarding the metal fuel relocation with pressure injection is necessary to find the effect of pressure on fuel fragmentation, penetration and dispersion in the coolant channel.

4. Conclusions

Experiments dropping molten uranium into test sections of single fuel pin geometry filled with sodium were conducted to investigate relocation behavior of metallic fuel in core structures of sodium-cooled fast reactors in case of HCDAs. The fuel cladding was disrupted due to eutectic formation between the uranium and the HT-9M for all experiments. The extent of eutectic formation increased with increasing molten uranium temperature. Voids formed by the boiling of sodium in coolant channel were also observed in the relocated fuel for all experiments. In case of the experiment #2, numerous fragments of the relocated fuel were found. The temperature profile as a function of time at the eutectic formation region above the weak spot was numerically calculated to evaluate the breach moment of the fuel cladding. Based on the numerical calculation, it could be concluded that the breach of the fuel cladding and the subsequent sodium boiling occurred within a few seconds from the drop moment. Generally, the instantaneous contact temperature of the present study was comparable to those of previous studies but the Weber number of the present study was relatively small compared to those of previous studies due to the narrow sodium channel. The difference of the instantaneous contact temperature between the experiment #1 and the experiment #2 resulted in the difference of the occurrence of the fragmentation. It could be concluded that the injected metallic uranium fuel is able to be fragmented and dispersed in the narrow coolant channel by the sodium boiling.

Acknowledgements

The authors are grateful for the MUSE facility design support from Stanley Wiedmeyer, Dennis Kilsdonk, and Arthur E. Wright at Argonne National Laboratory. They would like to acknowledge the helpful guidance and discussion on SFR accident analysis of Adrian M. Tentner and David Grabaskas at Argonne National Laboratory. This work was performed under the Cooperative Research and Development Agreement (CRADA) No. 1501601 supported by the Korea Atomic Energy Research Institute.

References

[1] Planchon, H.P., Singer, R.M., Mohr, D., Feldman, E.E., Chang, L.K. and Betten, P.R., 1986. The experimental breeder reactor II inherent shutdown and heat removal tests—results and analysis. Nuclear Engineering and Design, 91(3), pp.287-296.

[2] Chang, Y.I., 2007. Technical rationale for metal fuel in fast reactors. Nuclear Engineering and Technology, 39(3), pp.161-170.

[3] Nishimura, S., Kinoshita, I., Sugiyama, K.I. and UEDA, N., 2002. Thermal fragmentation of a molten metal jet dropped into a sodium pool at interface temperatures below its freezing point. Journal of nuclear science and technology, 39(7), pp.752-758.

[4] Nishimura, S., Kinoshita, I., Sugiyama, K.I. and Ueda, N., 2005. Thermal interaction between molten metal jet and sodium pool: effect of principal factors governing fragmentation of the jet. Nuclear technology, 149(2), pp.189-199.

[5] Nishimura, S., Zhang, Z.G., Sugiyama, K.I. and Kinoshita, I., 2007. Transformation and fragmentation behavior of molten metal drop in sodium pool. Nuclear Engineering and Design, 237(23), pp.2201-2209.

[6] Zhang, Z.G., Sugiyama, K.I., Itagaki, W., Nishimura, S., Kinosita, I. and Narabayashi, T., 2009. Fragmentation of a single molten metal droplet penetrating sodium pool I Copper droplet and the relationship with copper jet. Journal of nuclear science and technology, 46(5), pp.453-459.

[7] Zhang, Z.G. and Sugiyama, K.I., 2010. Fragmentation of a Single Molten Metal Droplet Penetrating Sodium Pool II Stainless Steel and the Relationship with Copper Droplet. Journal of nuclear science and technology, 47(2), pp.169-175.

[8] Gabor, J.D., Purviance, R.T., Aeschliman, R.W. and Spencer, B.W., 1987. Characterization of IFR metal fuel fragmentation. Trans. Am. Nucl. Soc.;(United States), 54(CONF-870601-).

[9] Gabor, J.D., Purviance, R.T., Aeschliman, R.W. and Spencer, B.W., 1989. DE89 017679 Dispersion and Thermal Interactions of Molten Metal Fuel Settling on A Horizontal Steel Plate through A Sodium Pool.

[10] Kamiyama, K., Saito, M., Matsuba, K.I., Isozaki, M., Sato, I., Konishi, K., Zuyev, V.A., Kolodeshnikov, A.A. and Vassiliev, Y.S., 2013. Experimental study on fuel-discharge

behavior through in-core coolant channels. Journal of Nuclear Science and Technology, 50(6), pp.629-644.

[11] Heo, H., Park, S.D., Jeong, D.W. and Bang, I.C., 2016. Visual study of ex-pin phenomena for SFR with metal fuel under initial phase of severe accidents by using simulants. Journal of Nuclear Science and Technology, 53(9), pp.1409-1416.

[12] Bauer, T.H., Wright, A.E., Robinson, W.R., Holland, J.W. and Rhodes, E.A., 1990. Behavior of modern metallic fuel in treat transient overpower tests. Nuclear technology, 92(3), pp.325-352.

[13] Walter, C.M. and Kelman, L.R., 1966. The interaction of iron with molten uranium. Journal of Nuclear Materials, 20(3), pp.314-322.

[14] Lee, K.L., Ha, K.S., Jeong, J.H., Choi, C.W., Jeong, T., Ahn, S.J., Lee, S.W., Chang, W.P., Kang, S.H. and Yoo, J., 2016. A Preliminary Safety Analysis for the Prototype Gen IV Sodium-Cooled Fast Reactor. Nuclear Engineering and Technology, 48(5), pp.1071-1082.

[15] Tentner, A., Kang, S., Karahan, A., 2017. Advances in the Development of the SAS4A Code Metallic Fuel Models for the Analysis of Prototype Gen-IV Sodium-cooled Fast Reactor Postulated Severe Accidents. International Conference on Fast Reactors and Related Fuel Cycles FR17, Yekaterinburg, Russian Federation.

Table 1. Parameters of the metal fuel relocation experiments performed in this study.

Experiment Number	Injection Velocity (m/s)	Injection Diameter (mm)	Weber Number	Fuel Material	Cladding Material	Initial Fuel Temperature at TC1 (°C)	Sodium Temperature (°C)	Fuel Amount (g)
1	1.4	3.175	5.2	Uranium	HT-9M	1248	501	212.37
2	1.7	3,175	3.5	Uranium	HT-9M	1333	622	308.76

Table 2. Instantaneous contact temperature and ambient Weber number of simulant and real fuel materials.

	Fuel Material	Melt Temperature (°C)	Sodium Temperature (°C)	Instantaneous Contact Interface Temperature (°C)	Ambient Weber Number
Nishimura [3-5]	Copper	1102-1282	280	995-1054	N/A
	Copper	1099-1249	206-500	975-1047	14-88
	Silver	966-1202	243-252	907-948	23-33
	Aluminum	677-1279	271-364	634-940	46-203
Zhang [6,7]	304 SS	1470-1820	295-337	901-1086	56-95
	Copper	1084-1718	249-314	867-1342	52-114
Gabor [8,9]	Uranium	1232	600	836	54
	Uranium	1532	600	948	
Present Study, Experiment #1	Uranium	1166	501	710	5.2
Present Study, Experiment #2	Uranium	1320	622	869	3.4

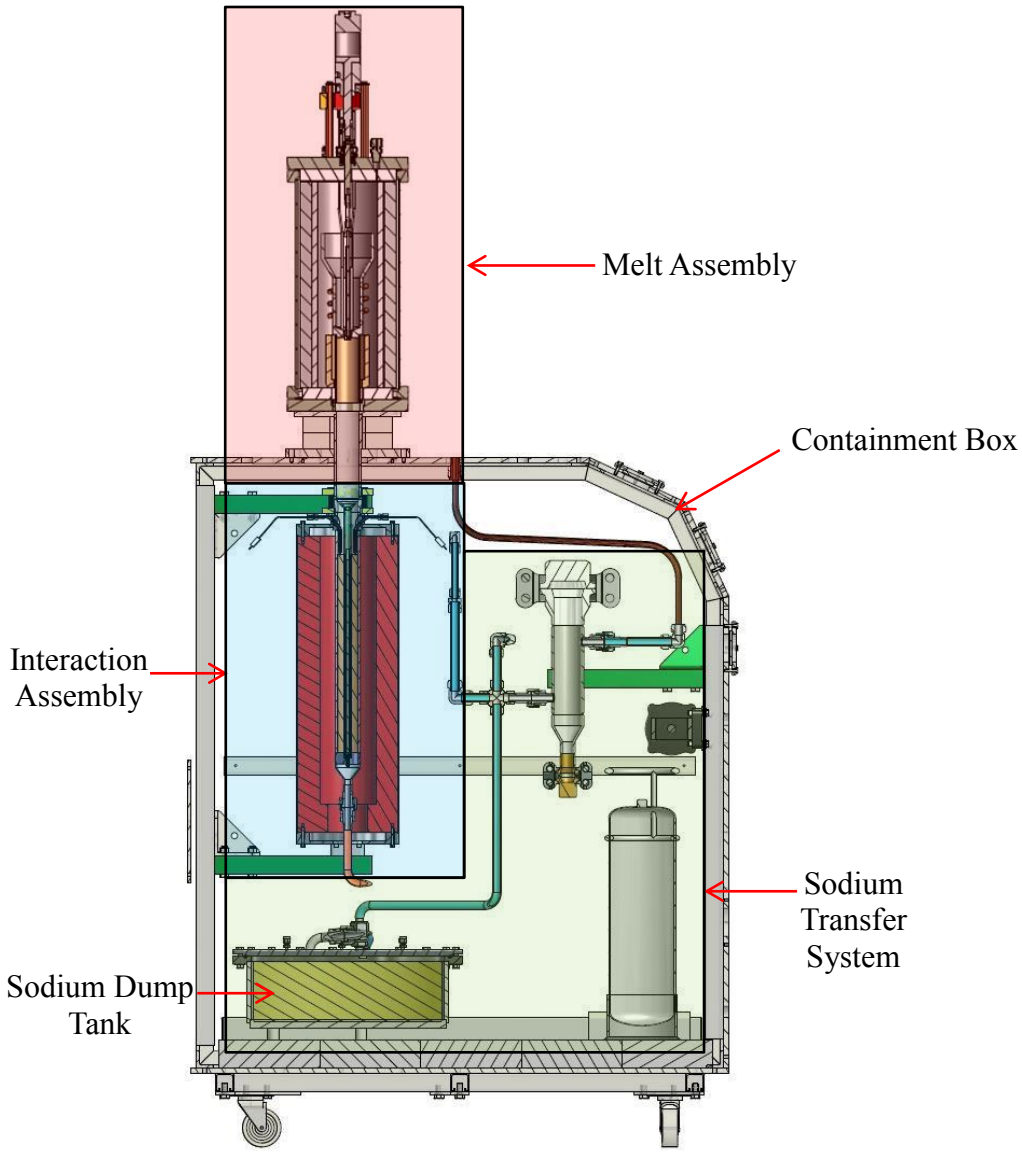

Figure 1. Schematic diagram of Metallic Uranium Safety Experiment (MUSE) facility

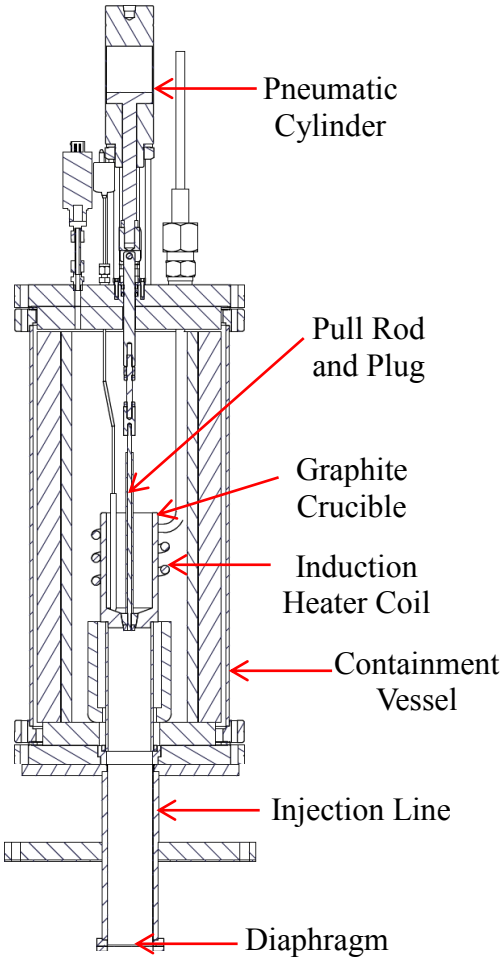

Figure 2. Schematic diagram of melt assembly

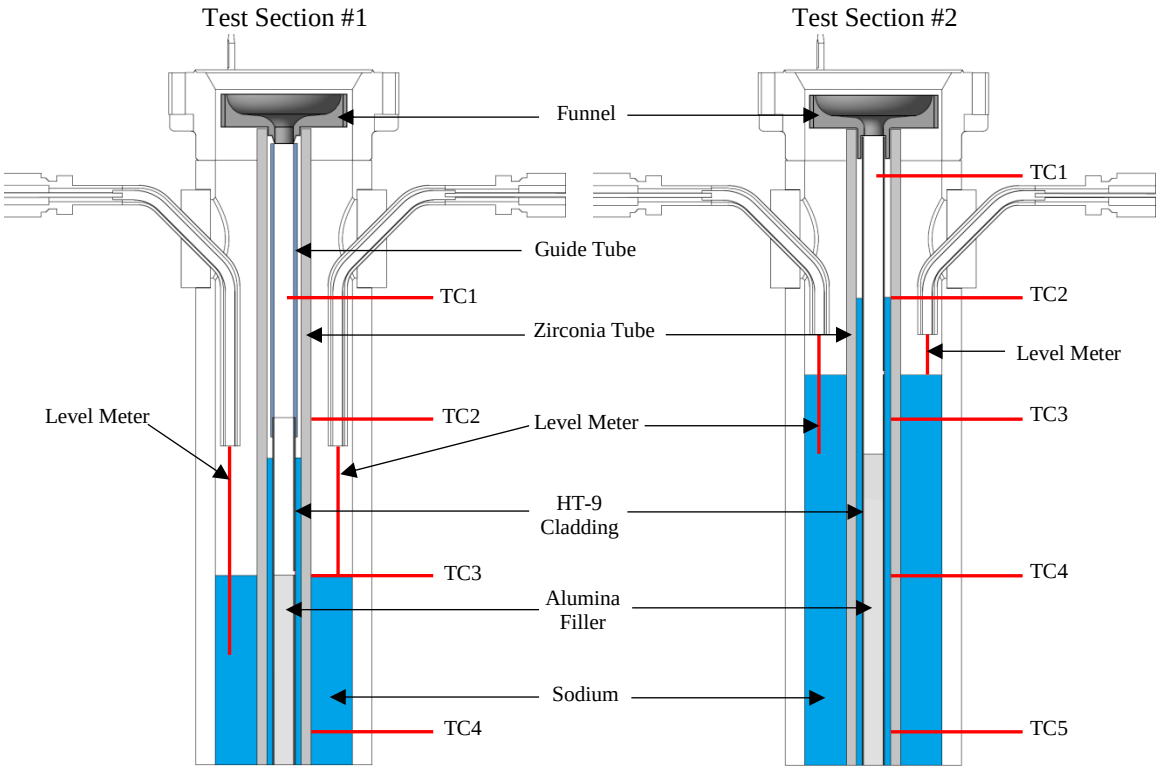

Figure 3. Schematic diagram of test sections

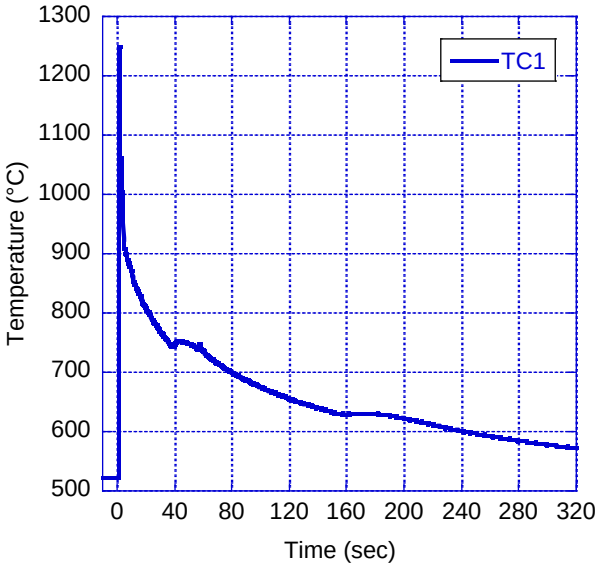

(a)

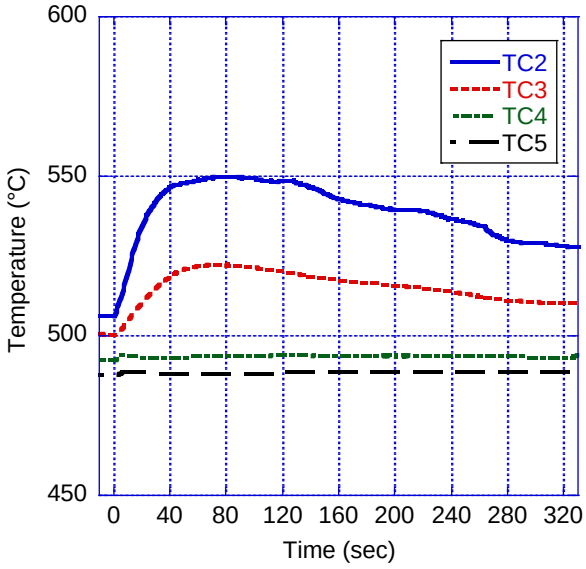

(b)

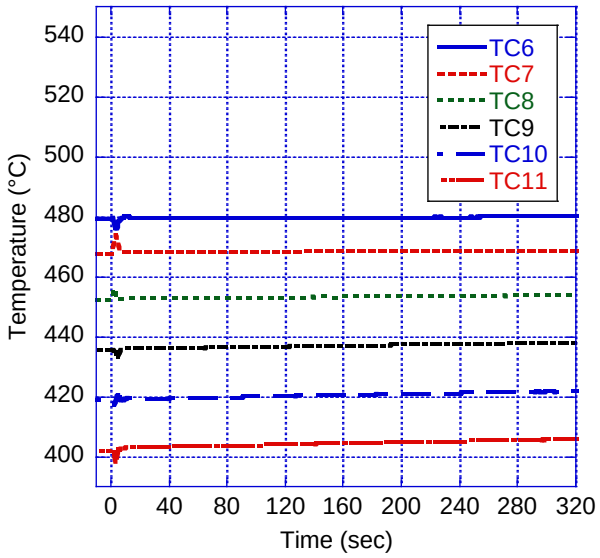

(c)

Figure 4. Temperature measurements of experiment #1: (a) TC1, (b) TC2 – TC5, (c) TC6 – TC11 (The limit of error of TC1-TC12 was 0.75%)

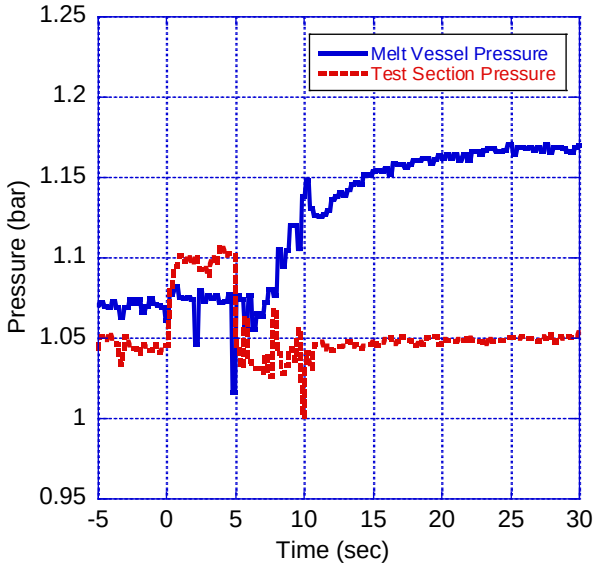

Figure 5. Pressure measurements of experiment #1

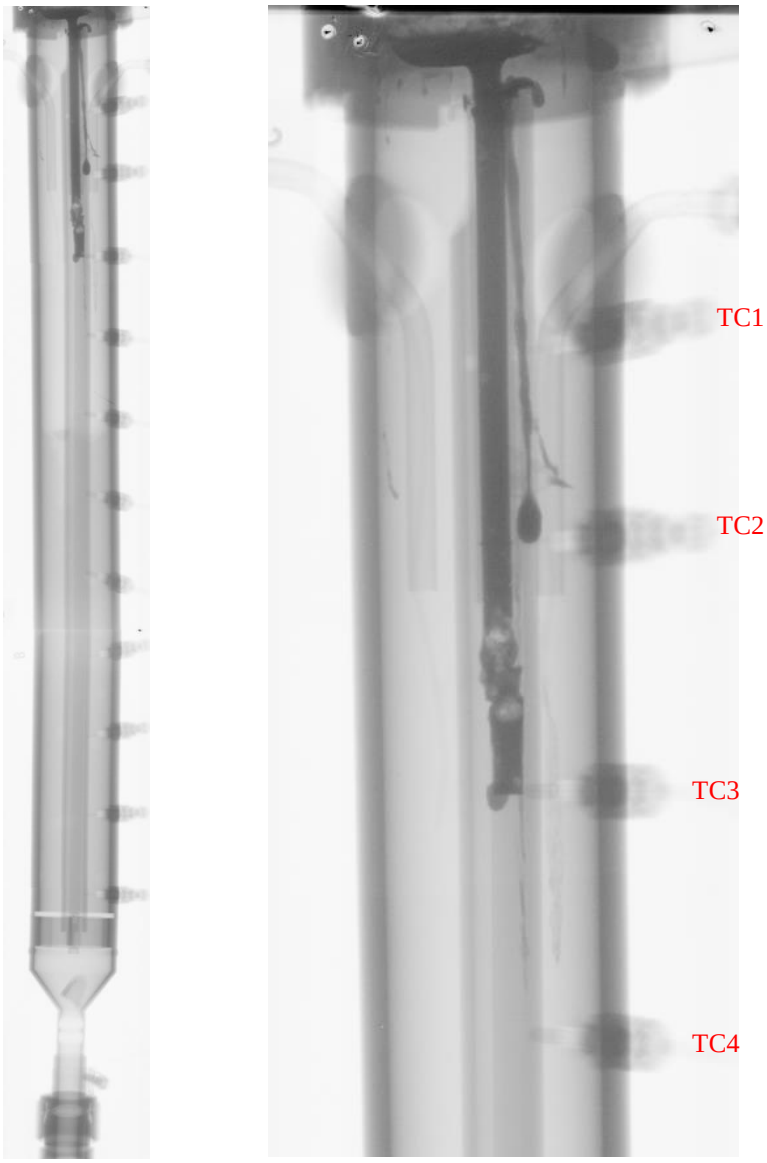

Figure 6. Posttest radiographic images of test section #1

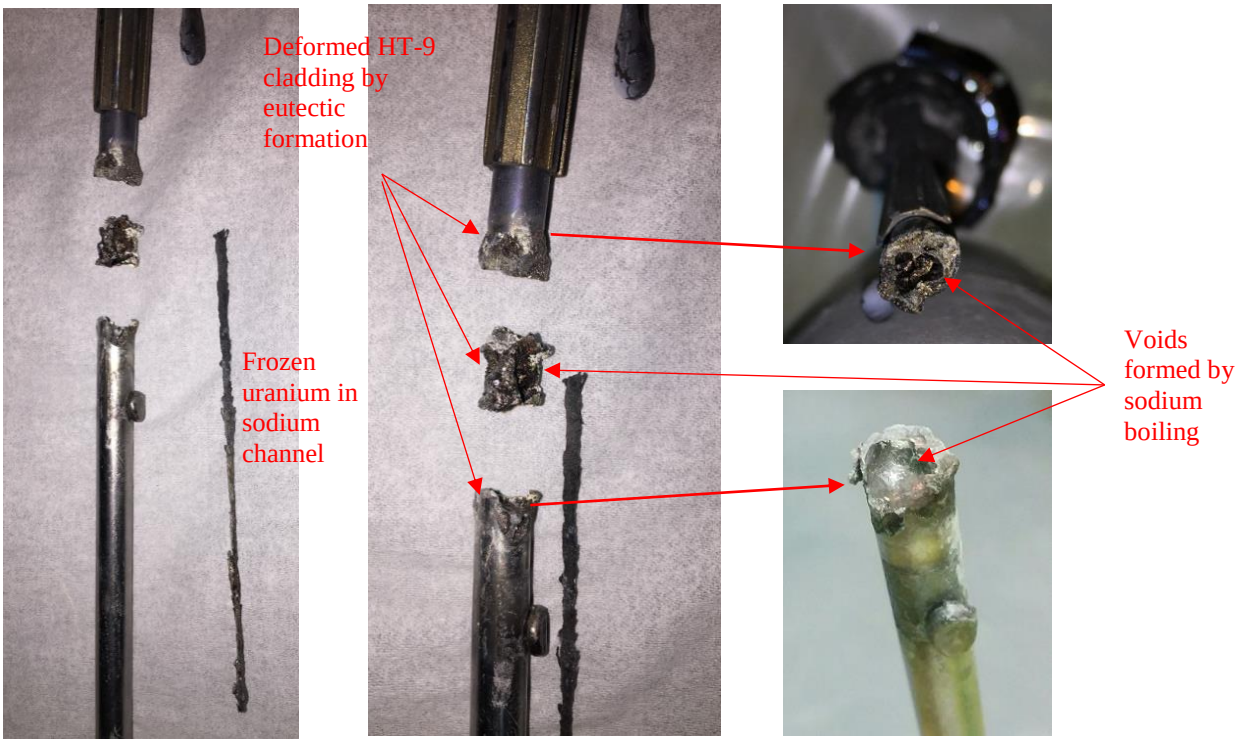

Figure 7. Disassembled test section #1

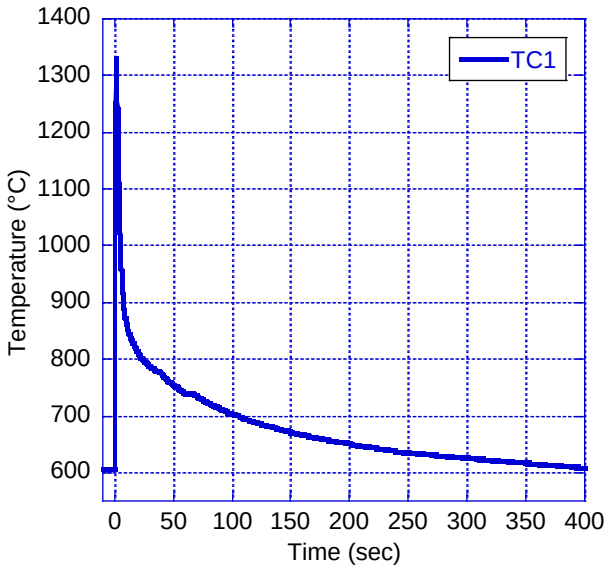

(a)

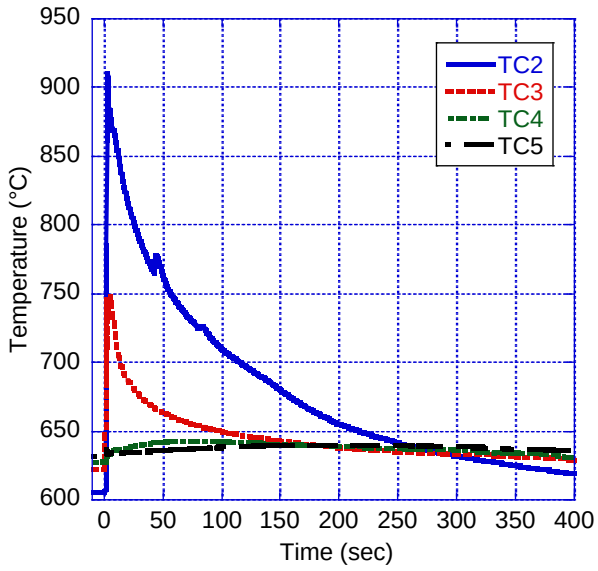

(b)

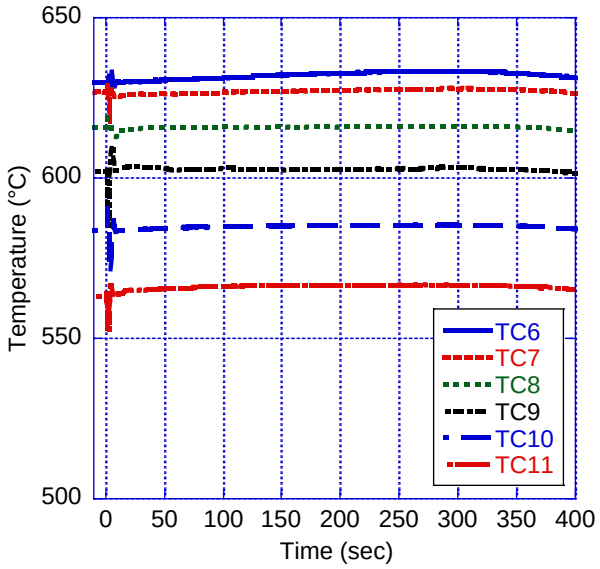

(c)

Figure 8. Temperature measurements of experiment #2: (a) TC1, (b) TC2 – TC5, (c) TC8 – TC11 (The limit of error of TC1 was 0.25% and the limit of error of TC2-TC12 was 0.75%)

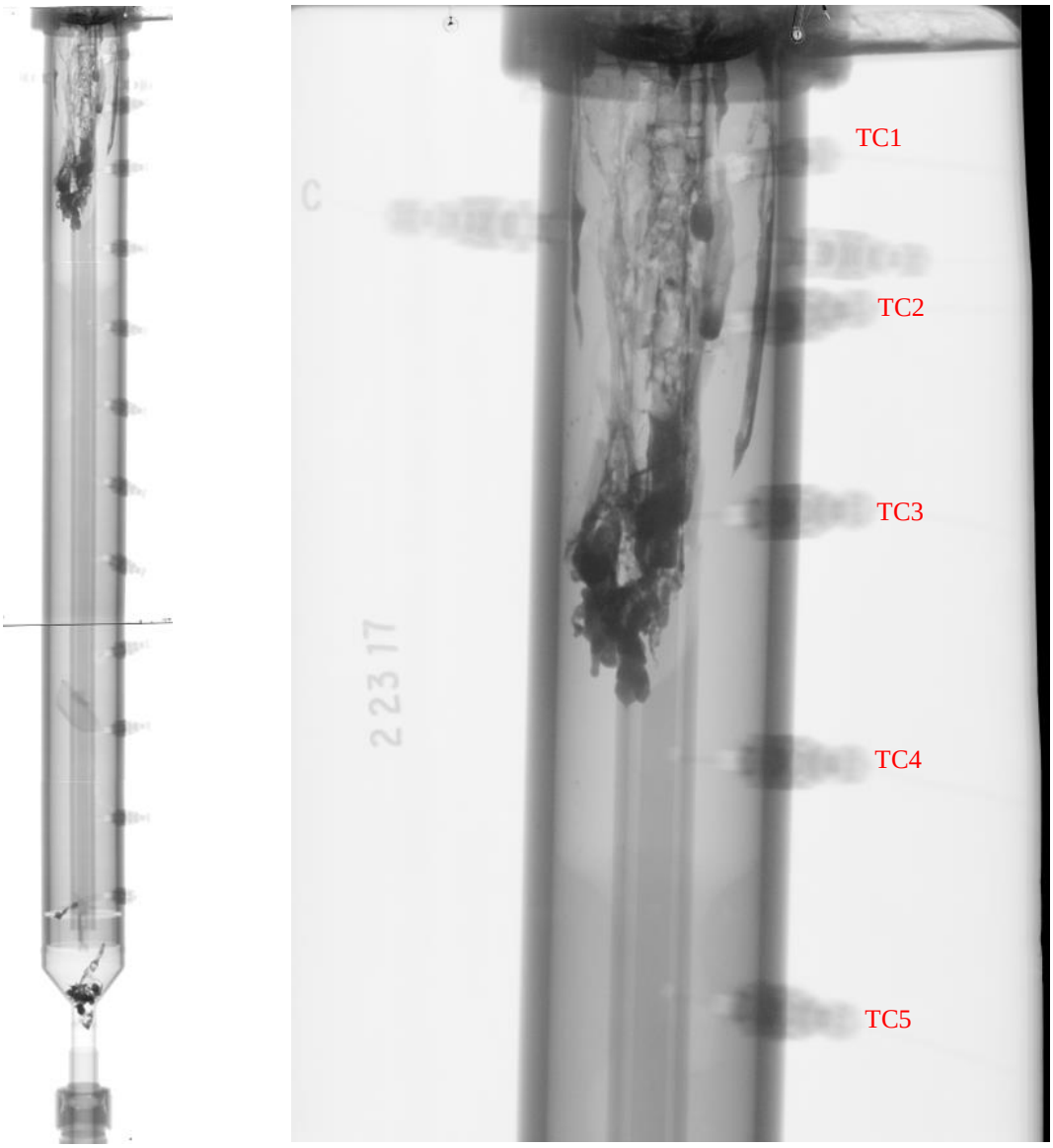

Figure 9. Posttest radiographic images of test section #2

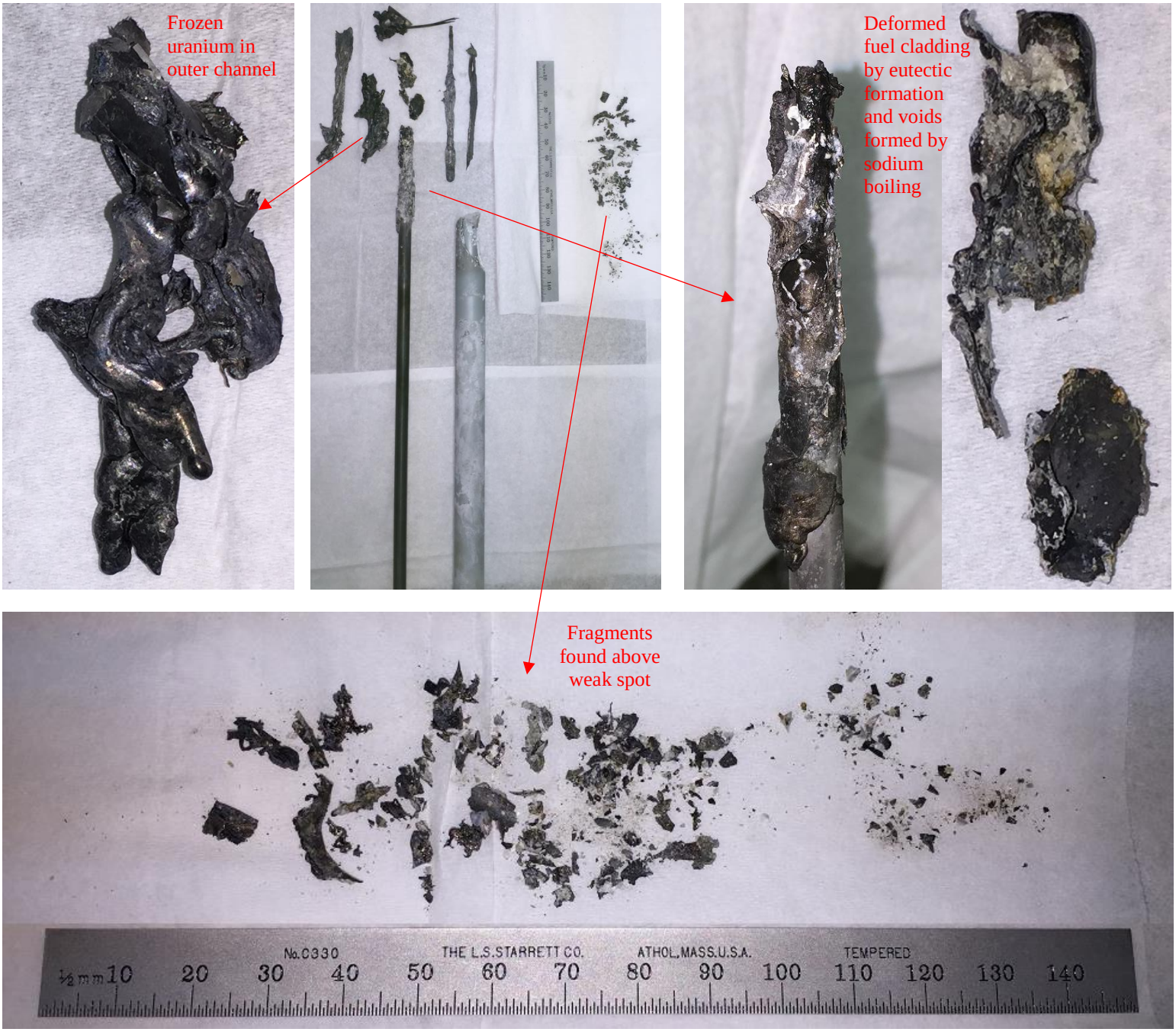

Figure 10. Disassembled test section #2

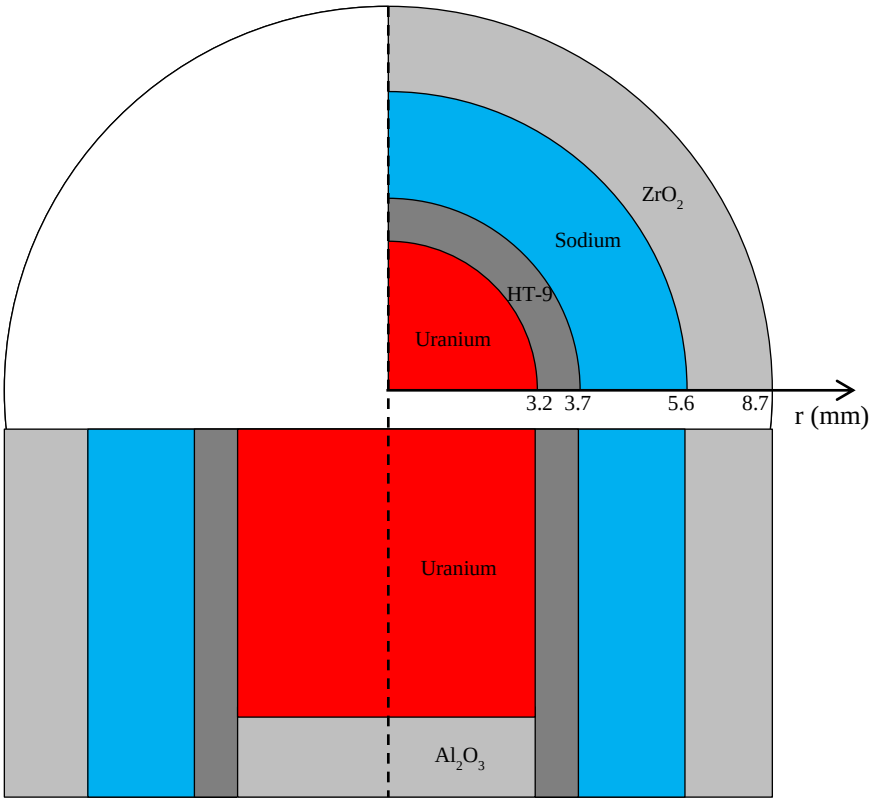

Figure 11. Cross sectional view of test section

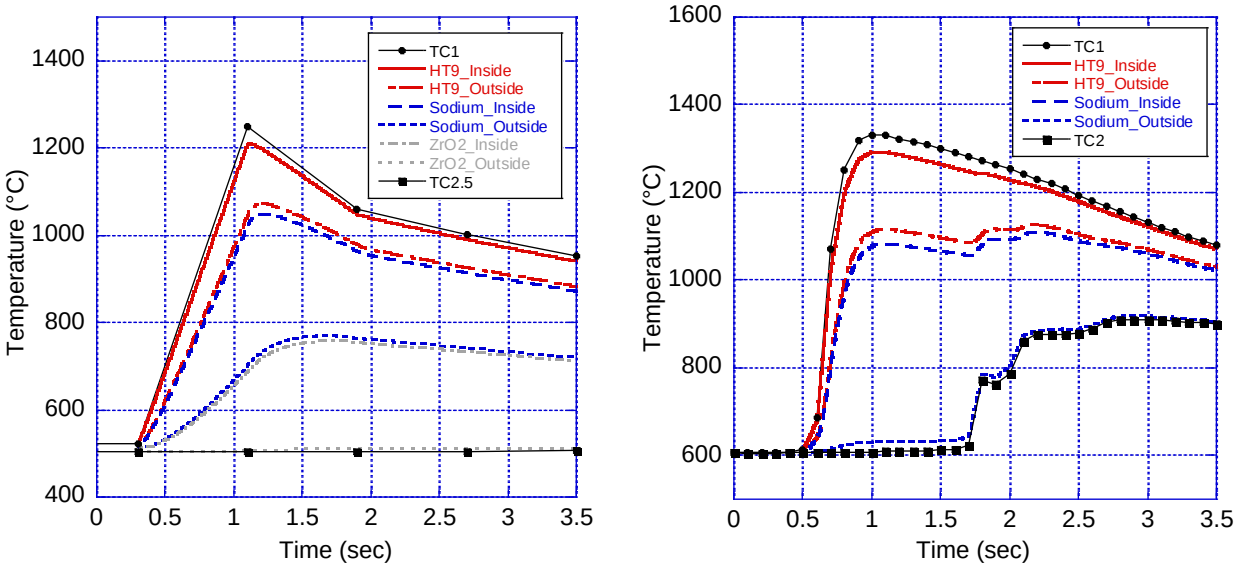

(a) (b)

Figure 12. Calculated temperature profile: (a) experiment #1 (b) experiment #2